© 2016. Published by The Company of Biologists Ltd | Development (2016) 143, 2183-2193 doi:10.1242/dev.128629

RESEARCH ARTICLE

Syk kinases are required for spinal commissural axon repulsion at the midline via the ephrin/Eph pathway

Nelly Noraz[1,2,3,‡], Iness Jaaoini[1,2,3], Camille Charoy[1,2,3], Chantal Watrin[1,2,3], Naura Chounlamountri[1,2,3], Aurélien Benon[1,2,3], Céline Malleval[1,2,3], Hélène Boudin[5], Jérôme Honnorat[1,2,3,4], Valérie Castellani[1,2,3,*] and Véronique Pellier-Monnin[1,2,3,*]

ABSTRACT

In the hematopoietic system, Syk family tyrosine kinases are essential components of immunoreceptor ITAM-based signaling. While there is increasing data indicating the involvement of immunoreceptors in neural functions, the contribution of Syk kinases remains obscure. Previously, we identified phosphorylated forms of Syk kinases in specialized populations of migrating neurons or projecting axons. Moreover, we identified ephrin/Eph as guidance molecules utilizing the ITAM-bearing CD3zeta (Cd247) and associated Syk kinases for the growth cone collapse response induced *in vitro*. Here, we show that in the developing spinal cord, Syk is phosphorylated in navigating commissural axons. By analyzing axon trajectories in open-book preparations of *Syk*$^{-/-}$; *Zap70*$^{-/-}$ mouse embryos, we show that Syk kinases are dispensable for attraction towards the midline but confer growth cone responsiveness to repulsive signals that expel commissural axons from the midline. Known to serve a repulsive function at the midline, ephrin B3/EphB2 are obvious candidates for driving the Syk-dependent repulsive response. Indeed, Syk kinases were found to be required for ephrin B3-induced growth cone collapse in cultured commissural neurons. In fragments of commissural neuron-enriched tissues, Syk is in a constitutively phosphorylated state and ephrin B3 decreased its level of phosphorylation. Direct pharmacological inhibition of Syk kinase activity was sufficient to induce growth cone collapse. In conclusion, Syk kinases act as a molecular switch of growth cone adhesive and repulsive responses.

KEY WORDS: Syk kinases, Ephrin/Eph, Neural tube, Commissural axons, Repulsion

INTRODUCTION

The function of the non-receptor spleen tyrosine kinase (Syk) family members Syk and Zap70 (also known as ZAP-70) has been well characterized in cells of the hematopoietic lineage. They relay signals emanating from classical immunoreceptors such as TCR, BCR, NKR and FcR, thereby controlling their homeostasis and functional outcome. Immunoreceptors utilize a common signal transduction mechanism, which relies on conserved immunoreceptor tyrosine-based activation motifs (ITAMs) that are mostly present in the signal transducing subunits or as part of the recognition subunits themselves. Immunoreceptors can act as either activator when present with ITAMs or as inhibitor when present with immunoreceptor tyrosine-based inhibition motifs (ITIMs). ITAM-based signaling depends on the coordinated interplay of the Src and Syk kinase families. Upon ligand recognition and receptor clustering, tyrosines within the ITAM are dually phosphorylated by Src family kinases, providing a docking site for the tandem SH2 domains of the Syk family kinases. These early events allow the recruitment and activation of both kinase families and serve as a crucial link to adapter molecules [e.g. Lat and SLP-76 (Lcp2)] capable of organizing multiple signaling pathways in a spatiotemporal manner. Downstream signaling ensues principally via the Ras, DAG and calcium-dependent signaling pathways, as well as via actin dynamics regulatory molecules (Smith-Garvin et al., 2009).

Importantly, ITAM-based signaling has been extended to non-immunoreceptors. Indeed, many cell surface molecules that are not restricted in expression to hematopoietic cells have been shown to signal through an immunoreceptor-like pathway. These principally comprise adhesion molecules implicated in cell-pathogen, cell-cell or cell-extracellular matrix (ECM) interactions or receptors linked to inflammatory adaptive responses. Some of them contain an ITAM on their own cytoplasmic tail but most, lacking such a motif, use an ITAM-transducing subunit in a co-optive manner to recruit and activate the Src/Syk kinases (Abram and Lowell, 2007; Ivashkiv, 2009; Kazerounian et al., 2011; Letellier et al., 2010). A striking feature of the diverse receptors utilizing ITAM-based signaling is their interplay with integrins at two intersected levels of regulation, referred as inside-out and outside-in (Jakus et al., 2007; Luckashenak and Clements, 2007). Overall, it appears that ITAM-based signaling typically does not function in isolation. Instead, it is enmeshed in the molecular network controlling cellular adhesion and chemotaxis as well as the functional outcome.

An increasing amount of data supports the involvement of ITAM- or ITIM-bearing molecules in neuronal functions, including dendrite and synapse formation, synaptic plasticity and behavior (Angibaud et al., 2012; Baudouin et al., 2008; Boulanger, 2009; Chuang and Lagenaur, 1990; Hamada et al., 2004; Kaifu et al., 2003; Kitano et al., 2002; Ogawa et al., 2007; Xu et al., 2010; Yamada et al., 2001). Consistent with a role for ITAM-based signaling in developmental events contributing to the establishment of neuronal connectivity, we showed in a previous study that Syk is phosphorylated on tyrosine residues representative of an active form of the kinase in regions of synaptogenesis and in specialized populations of migrating cells or projecting axons (Hatterer et al., 2011). Notably, since neurons are devoid of classical immunoreceptors, the neuronal function of ITAM-based signaling

[1]INSERM U1217, Institut NeuroMyoGène, Lyon F-69000, France. [2]CNRS UMR5310, Institut NeuroMyoGène, Lyon F-69000, France. [3]University Claude Bernard Lyon 1, Lyon F-69000, France. [4]Hospices Civils de Lyon, Lyon F-69000, France. [5]INSERM U1064, Institut de Transplantation Urologie-Néphrologie, Nantes F-44035, France.
*These authors contributed equally to this work

[‡]Author for correspondence (nelly.noraz@inserm.fr)

N.N., 0000-0003-4076-9773

Received 28 July 2015; Accepted 15 April 2016

Development (2016) 143, 2183-2193 doi:10.1242/dev.128629

is likely to be linked to unrelated receptors that use it in a co-optive manner. Interestingly, we identified ephrin/Eph as adhesion molecules utilizing CD3zeta (also known as Cd247) as an ITAM-transducing subunit for the growth cone collapse response *in vitro*. Stimulation of hippocampal neurons with ephrin A1 induces the translocation of CD3zeta and associated Syk tyrosine kinases to EphA4 receptor clusters. In addition, genetic disruption of CD3zeta confers a non-permissive background to ephrin A1-induced repulsive signals in these cells (Angibaud et al., 2011).

In the nervous system, to form precise neuronal networks axons navigate through a complex environment guided by the concerted action of guidance molecules. Eph receptor tyrosine kinases and their membrane-bound ligands, the ephrins, have been shown to play a crucial role in the processes of axon targeting. This arises from their ability to regulate cell-cell interactions, generating adhesive and repulsive responses (Egea and Klein, 2007; Pasquale, 2008). In the immune system, ephrin/Eph-associated functions fit well with the extended ITAM-based paradigm. Ephrin/Eph interactions positively or negatively regulate leukocyte adhesive properties as well as chemotactic responses (Funk and Orr, 2013). In addition, ephrin/Eph signaling affects leukocyte functional outcomes relying on classical immunoreceptors, including TCR-induced proliferation (Mendes-da-Cruz et al., 2012). They moreover interplay with other adhesion molecules, including integrins (Arvanitis and Davy, 2008; Pitulescu et al., 2010; Sharfe et al., 2008).

In light of these findings, we have studied the role of Syk kinases during spinal cord midline crossing, a well-characterized model of axon guidance in which ephrin/Eph have been implicated (Kadison et al., 2006).

RESULTS

Syk is phosphorylated in projecting commissural axons of E11-13 mouse embryos

In the developing mouse spinal cord, commissural axons project from the dorsal region to the floor plate and cross it before projecting to their contralateral synaptic targets in the caudorostral axis. This crossing decision is under exquisite spatial and temporal regulation. Growing commissural axons initially respond to attractive signals, but once across the floor plate repulsion dominates, allowing axons to leave and preventing them from re-entering the floor plate (Dickson and Zou, 2010).

To gain insight into the phosphorylation status of Syk kinases during this process, transverse sections of E11.5 and E13.5 embryos were stained with anti-βIII tubulin, a marker of differentiating neurons, and two antibodies recognizing phosphorylated forms of Syk Y525/526 and Syk Y352/Zap70 Y319. Notably, phosphorylation on these tyrosines has been shown to support an activator role (Brdicka et al., 2005; Zhang et al., 2000). The two phosphorylation-specific antibodies presented a similar pattern of labeling on E11.5 and E13.5 embryos (Fig. 1A,B; N.N., unpublished). Phospho-Syk/Zap70 labeling was readily detected in different axonal populations comprising commissural axons, sensory nerve fibers in the dorsal root entry zone and motor axons originating from the developing motor columns. A similar pattern of expression was also obtained using Syk/Zap70-specific antibodies but with much lower intensity (N.N., unpublished). No obvious staining was observed in control conditions (Fig. 1C). In commissural neurons, Syk kinases appeared phosphorylated in precrossing axons extending from the cell bodies residing in the

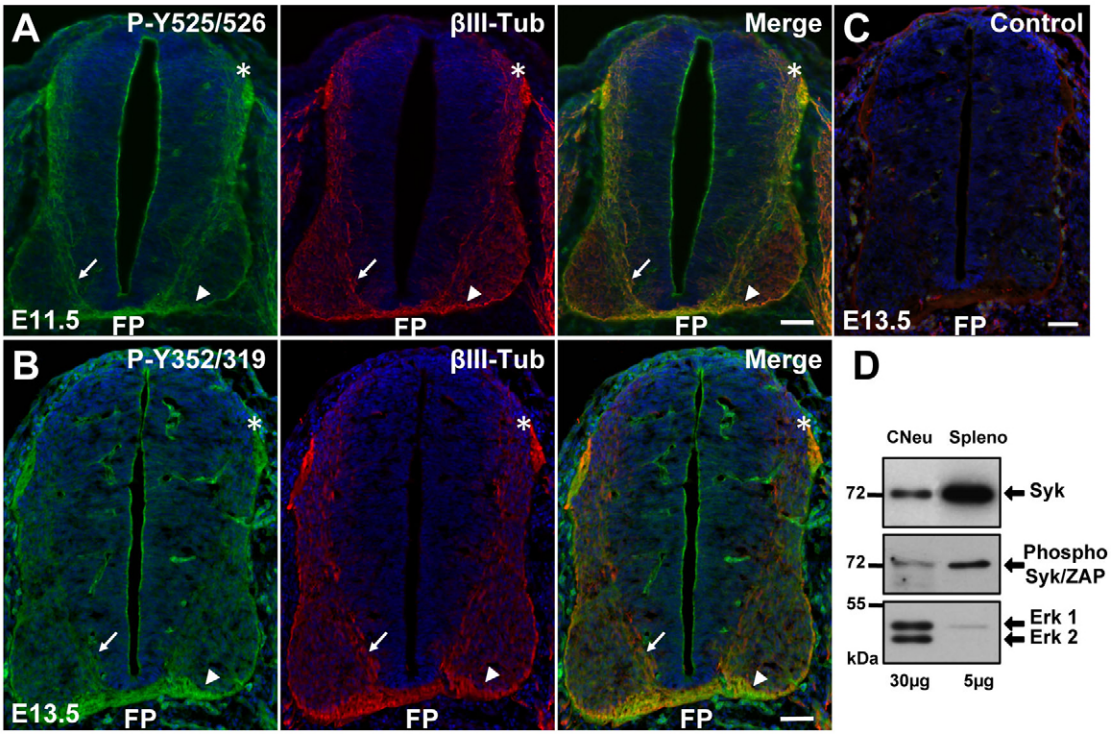

Fig. 1. Syk kinases are phosphorylated in outgrowing commissural axons. (A,B) Transverse sections of E11.5 (A) and E13.5 (B) mouse spinal cords were immunostained for phospho-Syk (P-Y525/526) or phospho-Syk/Zap70 (P-Y352/319) and βIII-tubulin. (C) Immunostaining in control conditions with omission of primary antibodies. Asterisk, dorsal root entry zone; arrow, precrossing axons; arrowhead, postcrossing axons. FP, floor plate. Scale bars: 50 µm. (D) Western blot performed on total tissue extracts obtained from the dorsal part of E12.5 open-book preparations (CNeu, 30 µg protein) and splenocytes of adult mice (Spleno, 5 µg protein). Membranes were blotted with anti-Syk (N19) and anti-phospho-Syk/Zap70 (P-Y352/319) antibodies. Erk1 and Erk2 were used as loading controls. CNeu, commissural neurons; spleno, splenocytes.

Development (2016) 143, 2183-2193 doi:10.1242/dev.128629

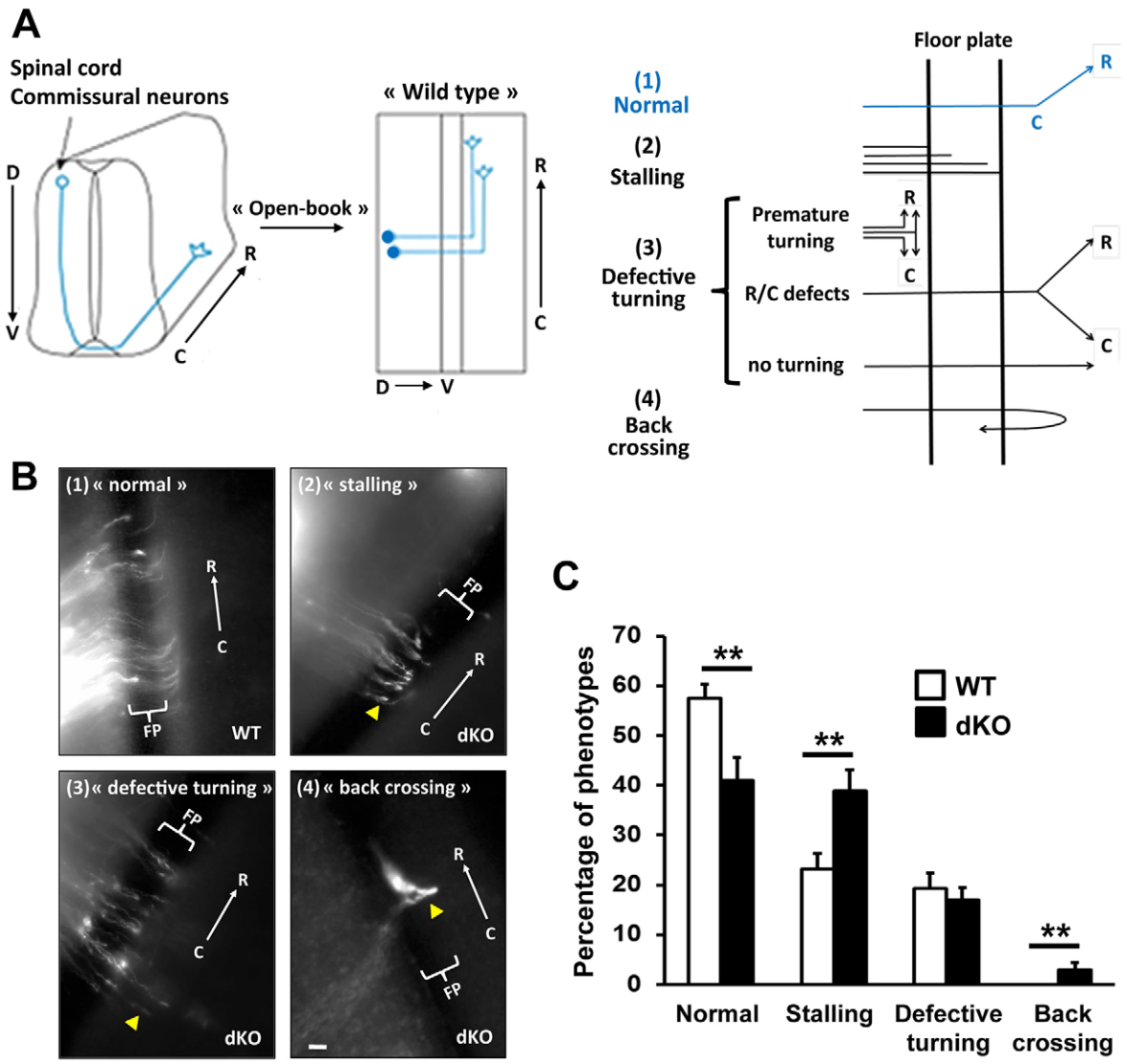

Fig. 2. Syk kinases are required to expel commissural axons from the midline. (A) Schematics of spinal cord open-book preparations with anterograde labeling of commissural axons after insertion of DiI crystals in the dorsal part. As observed on E13.5 WT and dKO open-book preparations, the different trajectories are represented as: (1) 'normal' when commissural axons crossed the floor plate and turned rostrally; (2) 'stalling' when commissural axons were arrested in the floor plate; (3) 'defective turning', which includes 'premature turning' when commissural axons turned prematurely before crossing the floor plate, 'R/C defects' when commissural axons turned in an aberrant rostrocaudal direction, and 'no turning' when commissural axons projected straight without turning after crossing the floor plate; and (4) 'back crossing' when commissural axons recrossed the floor plate. (B) Images illustrating examples of fiber tract trajectories observed from one inserted DiI crystal. Images are focused on axons crossing the floor plate, since most of abnormal trajectories (arrowheads) were observed at this particular step. As an example, in B phenotype (3), although several fiber tracts with a defective turning or a stalling phenotype are observed we counted one defective turning phenotype and one stalling phenotype. (C) For each open-book (embryo), the percentage of each phenotype was determined and results are represented as mean percentage±s.e.m. WT, *n*=21 embryos (84 crystals, 156 counted phenotypes); dKO, *n*=13 embryos (62 crystals, 143 counted phenotypes). Two-tailed Student's *t*-test, except for the back crossing phenotype for which a Mann–Whitney test was applied. ***P*<0.01. D, dorsal; V, ventral; C, caudal; R, rostral; FP, floor plate. Scale bar: 30 µm.

dorsal regions of the spinal cord, in crossing axons at the floor plate forming the ventral commissure, and in postcrossing axons coursing in the ventral as well as the lateral funiculi (Fig. 1A,B). Syk expression and phosphorylation were confirmed by western blot on tissue extracts prepared from the most dorsal part of E12.5 open-book preparations, enriched in commissural neurons (Fig. 1D).

Syk kinases are required *in vivo* to expel commissural axons from the midline

To investigate the role of Syk kinases in commissural axon guidance, we generated $Syk^{-/-}$; $Zap70^{-/-}$ double-knockout (dKO) mouse embryos. Whereas the *Zap70* knockout is viable and leads to a block in T cell differentiation at the $CD4^{+}$ $CD8^{+}$ double-positive stage (Kadlecek et al., 1998), *Syk* knockout mice die around birth with marked petechiae due to blood-lymphatic shunts, and fewer than 10% of $Syk^{-/-}$ mice survive postnatal day 2 (Turner et al., 1995). Therefore, $Syk^{-/-}$; $Zap70^{-/-}$ embryos were generated by intercrossing $Syk^{+/-}$; $Zap70^{-/-}$ animals and commissural axon trajectory was examined on E13.5 spinal cord open-book preparations. DiI crystals were applied to the most dorsal part of mutant or wild-type (WT) open-book preparations and after 2 days the trajectory of commissural axons was analyzed (Fig. 2A,B).

In dKO embryos, precrossing axons were apparently normally fasciculated and reached the midline. Moreover, they entered the

Development (2016) 143, 2183-2193 doi:10.1242/dev.128629

midline showing no significant premature turning or premature stalling/knotting. These observations indicated that the molecular machinery supporting growth cone dynamics is intact in Syk family kinase-deficient cells and that Syk kinases are dispensable for growth cone responsiveness to floor plate-derived attractive signals. By contrast, dKO embryos presented obvious late pathfinding errors (Fig. 2C). Compared with WT animals, the percentage of fiber tracts with a 'normal' pathfinding phenotype was significantly reduced in dKO embryos (57.5±2.9% versus 41.0±4.6%, $P<0.01$). The proportion of fiber tracts showing a 'defective turning' phenotype did not differ between the two groups ($P>0.05$). However, dKO embryos presented a higher percentage of fibers in 'stalling' (39.0±4.1% versus 23.0±3.5%, $P<0.01$) and, strikingly, 3.0±1.4% of them were observed to be 'back crossing', a phenotype never seen in WT animals. These results indicated that Syk kinases are required to expel commissural axons from the floor plate and to prevent them from recrossing the midline. Among the guidance molecules described in the literature as participating in such repulsive functions, namely Slits (Long et al., 2004), ephrins (Kadison et al., 2006) and semaphorins (Nawabi et al., 2010; Zou et al., 2000), we favored the ephrin/Eph pathway because we had data showing that, in hippocampal neurons, Syk kinases are involved in ephrin A1-induced growth cone collapse (Angibaud et al., 2011). On that basis, the possible involvement of Syk kinases downstream of the ephrin/Eph pathway in commissural neurons was explored.

Syk kinases are required for ephrin B3-induced growth cone collapse

In the developing spinal cord, ephrins are expressed in glial cells present at the floor plate and EphB receptors are expressed in commissural neurons (Imondi et al., 2000; Jevince et al., 2006). In addition, whereas similar crossing errors were reported in mice lacking EphB receptors (EphB1, EphB2 and EphB3) or ephrin B3, mice expressing a form of ephrin B3 truncated in its cytoplasmic domain, and thereby unable to transduce signals, presented no abnormalities (Kadison et al., 2006), thus confirming that EphB forward signaling rather than ephrin B3 reverse signaling controls commissural axon midline crossing. Besides, ephrin B3 acts on commissural neurons as a growth cone collapsing factor, as shown previously using E13 spinal cord explants (Imondi et al., 2000). Therefore, in a first set of experiments, an ephrin B3-induced growth cone collapse assay was set up. Recombinant ephrin B3-Fc was added to 48 h cell cultures of commissural neurons isolated from E12.5 or E13.5 WT spinal cords and, after 30 min, growth cone collapse was quantified (Fig. 3A). Since ephrin oligomerization is required for collapsing activity (Davis et al., 1994), ephrin B3-Fc recombinant proteins were clustered with an anti-Fc antibody before assaying. At basal level (Ctr), commissural neurons presented 26.9±5.4% collapsed growth cones, and the addition of the control, which comprises an Fc fragment only, did not change growth cone behavior (30.9±3.6%, $P>0.05$). By contrast, and as expected, the clustered ephrin B3 (eB3) but not the monomeric forms (eB3m) induced a marked collapse (eB3, 67.8±4.6% versus 30.9±3.6%, $P<0.001$; eB3m, 34.7±3.5% versus 30.9±3.6%, $P>0.05$). Notably, eB3 caused rapid growth cone collapse, reaching a maximum within 5 min, as demonstrated in the timecourse assay (Fig. 3B).

In a second set of experiments, the collapsing effect of ephrin B3 was assessed on commissural neurons isolated from dKO embryos. As shown in Fig. 3C, whereas 67.8±4.6% of growth cones were collapsed in WT cells after eB3 treatment, doubly deficient cells remained unresponsive with a collapse of 34.1±3.6%, similar to the control Fc condition of 36.7±12.8% ($P>0.05$). Such a defect was linked to Syk deficiency rather than to any particular feature of the genetic background, since in $Syk^{+/+}$; $Zap70^{-/-}$ mice from the same litter the response to eB3 was restored with 63.7±3.5% collapse ($P<0.001$). Neurons cultured from dKO embryos did not present any morphological peculiarities. Furthermore, the degree of spontaneous collapse observed in the control Fc condition (Fig. 3C), the culture content of Dcc^{+} cells (a marker of commissural neurons), as well as the cell viability were similar between dKO and WT animals (Fig. 3D). Taken together, these results showed that signaling via Syk kinases is required for ephrin B3-mediated commissural neuron growth cone collapse.

Syk kinases are involved in proximal events leading to ephrin B3 cleavage and/or ephrin B3/EphB2 endocytosis

Regarding the EphB receptor(s) mediating the repulsive function of ephrin B3 in commissural neurons, we identified EphB2 as one candidate. In spinal cord sections of E12.5 embryos, EphB2 labeling was found in commissural axons crossing the floor plate and its expression was confirmed by western blot on commissural neuron-enriched tissue extracts (Fig. 4A,B). EphB2 was also observed in commissural neurons cultured *in vitro*. The signal was detected in clusters of variable size distributed all over the surface of the cells (Fig. 4C, top) and was observed in the majority of cells. To address whether ephrin B3-induced growth cone collapse relies on EphB2, commissural neurons were treated with ephrin B3-Fc recombinant proteins preclustered with an anti-Fc biotinylated antibody. A double surface labeling was performed with Alexa 546-conjugated streptavidin to visualize the cell-bound eB3 fraction (red) and with anti-EphB2 primary plus anti-goat Alexa 488-conjugated secondary antibodies to visualize EphB2 receptor (green). After 5 min at 37°C, the cell-bound fraction of eB3 almost always colocalized with EphB2. Notably, both eB3 and EphB2 staining appeared as large dots representative of ephrin B3/EphB2 complex formation (Fig. 4C, middle panel). Such ephrin B3-induced EphB2 receptor clustering identified EphB2 as a clear candidate in mediating commissural neuron growth cone collapse. Nonetheless, EphB1 and EphB3, which have a similar pattern of expression to EphB2 on spinal cord sections (Imondi et al., 2000; Jevince et al., 2006), remain possible candidates.

In a number of assay systems, ephrin/Eph interactions have been shown to positively or negatively regulate growth cone adhesive properties. Importantly, both responses rely on Eph receptor clustering and are determined individually through receptor intracellular signaling. Adhesion is associated with low Eph kinase activity, prolonged ephrin binding and Eph clustering. By contrast, repulsion is associated with high Eph kinase activity, ephrin proteolytic cleavage and/or endocytosis, as well as cytoskeletal collapse of cell protrusions, both processes resulting in surface clearance of the ligand (Janes et al., 2012; Pasquale, 2005). In dKO neurons treated with eB3, collapse was impaired. A possible reason is a defect in the initial ephrin/Eph binding and clustering events. To address this possibility, WT and dKO neurons were treated as before and the state of collapse, as well as the number of eB3 clusters present on the growth cone surface, were compared. As expected, in WT cells, growth cone collapse was accompanied by rapid surface clearance of eB3 ligand (Fig. 4C, bottom) and was observed in the majority of cells, whereas prolonged eB3 binding and EphB2 clustering were a hallmark of the non-collapsed growth cones (Fig. 4C, middle). In cultures established from dKO embryos, most of the growth cones were non-collapsed but presented eB3 clusters at the cell surface. Importantly, the number of clusters that formed in neurons lacking Syk kinases was not significantly different from WT cells (14.15±1.50 in dKO versus 13.71±1.11 in WT for non-collapsed growth

Development (2016) 143, 2183-2193 doi:10.1242/dev.128629

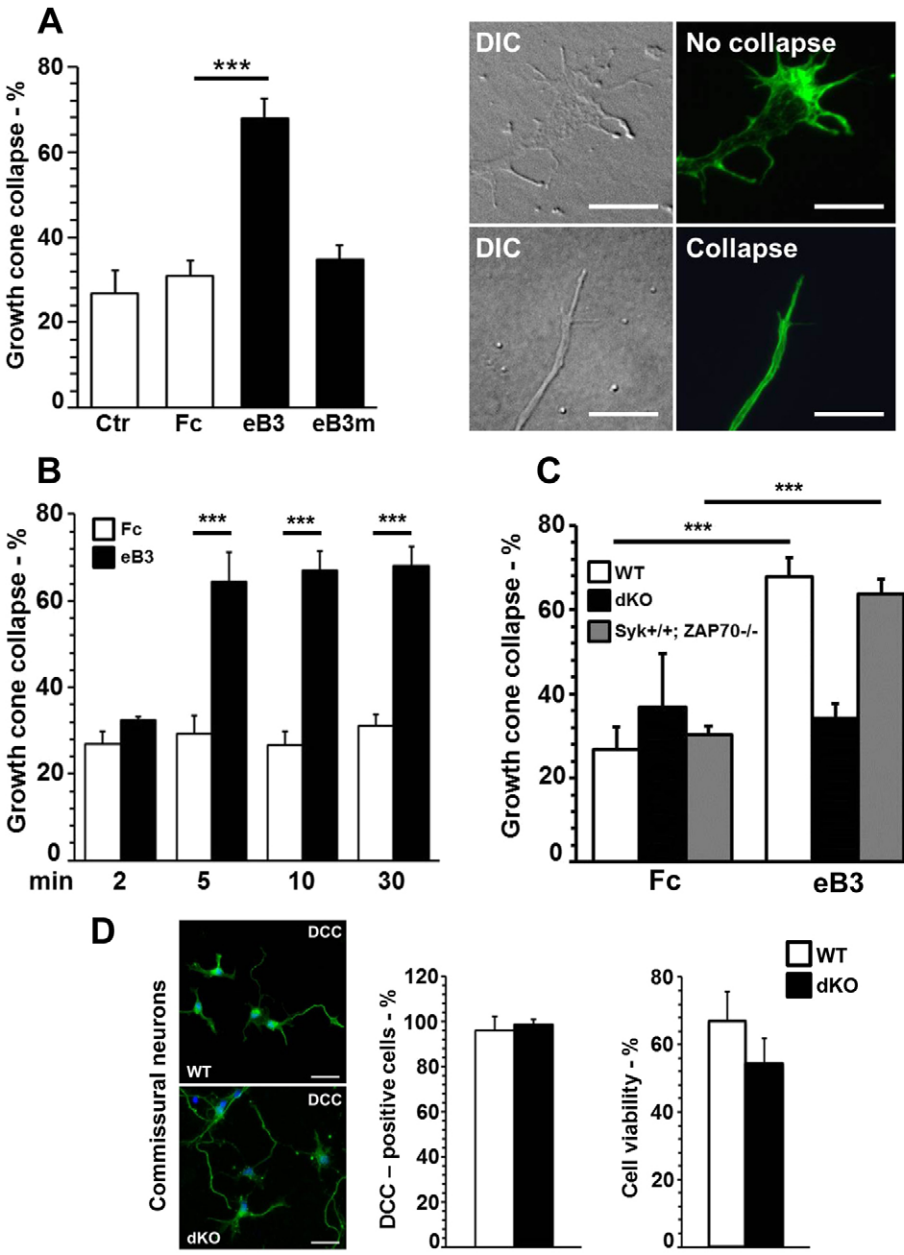

Fig. 3. Syk kinases are required for ephrin B3-induced growth cone collapse. (A) Cultures (48 h) of commissural neurons isolated from E12.5 WT spinal cords were treated for 30 min with culture medium (Ctr) or preclustered control Fc (Fc) and ephrin B3-Fc (eB3) or monomeric ephrin B3 (eB3m) at 0.5 µg/ml and growth cone collapse was quantified. Non-collapsed and collapsed growth cones labeled by phalloidin are illustrated on the right. (B) WT commissural neurons were treated as before with Fc or eB3 and growth cone collapse was assessed after 2, 5, 10 and 30 min. (C) Cultures of commissural neurons isolated from E12.5 WT, dKO or $Syk^{+/+}$; $Zap70^{-/-}$ spinal cords were treated with Fc and eB3 for 30 min and the percentage of collapsed growth cones determined. Experiments were performed in triplicate with at least 100 growth cones analyzed per coverslip and were repeated two or three times. (D) Cultures of commissural neurons isolated from E12.5 WT or dKO embryos were labeled with anti-Dcc antibodies and DAPI and the percentage of Dcc^{+} cells or viable cells determined. Experiments were repeated two or three times and more than 900 cells were analyzed for each experiment. All bar charts show mean percentage±s.d. Two-tailed Student's *t*-test. ***P<0.001. Scale bars: 10 µm in A; 20 µm in D.

cones, P>0.05; and 2.85±0.51 in dKO versus 1.17±0.23 in WT for collapsed growth cones, P>0.05; Fig. 4D), indicating that ephrin B3 binding and clustering occurred normally in dKO cells. In agreement with these observations, EphB2 was expressed normally in dKO embryos (Fig. 4A,B). To conclude, Syk kinases are dispensable for prolonged ephrin B3 binding and EphB2 clustering, which are likely to confer growth cone adhesive properties, but are instead involved in proximal signaling events leading to ephrin B3 cleavage and/or ephrin B3/EphB2 endocytosis.

We next asked whether EphB2 activation might be defective in dKO mice. Upon ephrin binding, Eph receptors become phosphorylated on tyrosine residues present in the juxtamembrane segment of the protein. Phosphorylation promotes kinase activity by disrupting intramolecular inhibitory interactions and generates docking sites for signaling partners, ultimately leading to repulsion (Pasquale, 2005). Therefore, the phosphorylation status of EphB2 upon ephrin B3 binding was examined in WT and dKO animals. Fragments of commissural neuron-enriched tissues freshly obtained from E12.5 open-book preparations were incubated for 5 min at 37°C with preclustered control Fc or ephrin B3-Fc (eB3) and protein lysates were blotted with anti-phospho-EphB2 juxtamembrane Y594 (Fig. 4E). As expected, eB3 led to a rapid increase in EphB2 phosphorylation in WT treated tissues. By contrast, in the absence of Syk kinases, the level of EphB2 phosphorylation remained unchanged. These findings indicate that, in dKO animals, axon guidance defects are associated with impaired EphB2 proximal signaling.

Ephrin B3-induced collapse is associated with a decrease in Syk phosphorylation

We next looked for changes in the level of Syk phosphorylation and/or its recruitment to EphB2 clusters upon ephrin B3 addition. Cultures were treated as before with control Fc or eB3 recombinant proteins, quickly washed, fixed and permeabilized. eB3 clusters were visualized using Alexa 488-conjugated streptavidin in green and

Development (2016) 143, 2183-2193 doi:10.1242/dev.128629

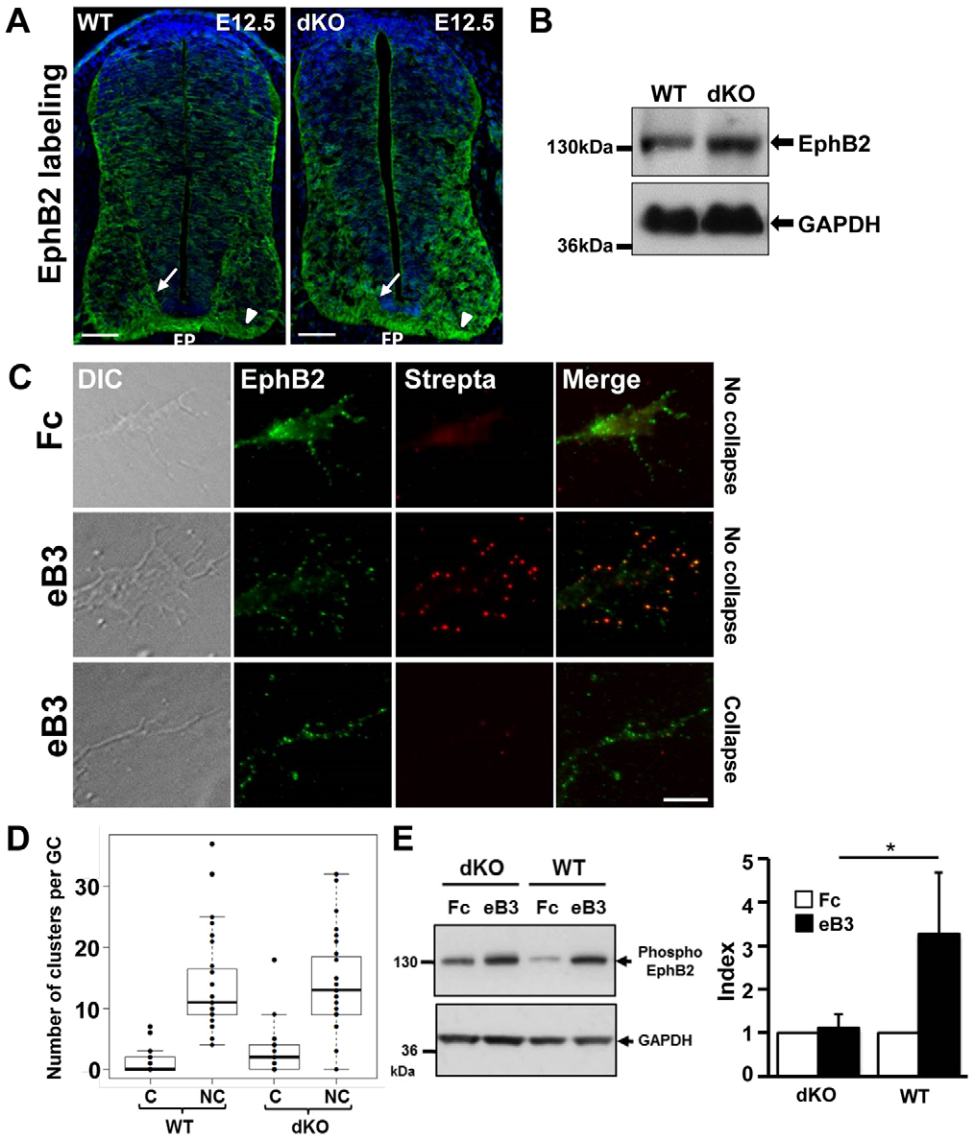

Fig. 4. Syk kinases are part of events leading to eB3 surface clearance. (A) EphB2 immunolabeling of spinal cord transverse sections of E12.5 WT and dKO mouse embryos. Arrow, precrossing commissural axons; arrowhead, postcrossing commissural axons. FP, floor plate. (B) Representative western blot illustrating EphB2 expression in commissural neuron-enriched tissue extracts of E12.5 WT and dKO embryos. Gapdh was used as loading control. (C) Commissural neurons isolated from E12.5 WT spinal cords were cultured for 48 h and treated for 5 min with Fc or eB3. Growth cone DIC images, with EphB2 receptor surface labeling (green) and eB3 bound fraction (streptavidin, red). (D) Quantitative analysis of the number of eB3 clusters present on the surface of collapsed (C) and non-collapsed (NC) growth cones (GC) in WT and dKO cultures treated as in C. Data resulting from three independent experiments are compiled in a box plot. Mann–Whitney test. (E) Western blot analysis of EphB2 Y594 phosphorylation in tissue extracts treated for 5 min with Fc or eB3. Quantification of signal intensities obtained from three independent experiments is depicted as mean index±s.d. Two-tailed Student's *t*-test. **P*<0.05. Scale bars: 50 µm in A; 20 µm in C.

phospho-Syk using anti-phospho-Syk Y348 primary with anti-mouse Alexa 555-conjugated secondary antibodies in red (Fig. 5A). In control Fc-treated cells, phospho-Syk was readily detected; staining appeared as puncta of various sizes and intensities distributed throughout the cell, as well as along the length and tip of filopodia (Fig. 5A, left). After eB3 treatment, the overall phospho-Syk signal intensity decreased, although in a non-significant manner (Fig. 5A, bar chart). eB3 clusters were found in close proximity to phospho-Syk labeling (Fig. 5A, right). However, since collapse was accompanied by a rapid surface clearance of ephrin B3, the proximity of phospho-Syk to EphB2-engaged receptor was essentially only observable on non-collapsed cells. Consequently, a link between the state of Syk phosphorylation and growth cone collapse could not be established using this approach.

To determine whether Syk activity was required for ephrin B3-mediated growth cone collapse, the experiment was repeated in the presence of 1 µM BAY 61-3606 (Bay-61), a pharmacological inhibitor that competes for the Syk ATP-binding site. Strikingly (Fig. 5B, left), WT neurons exposed to Syk inhibitor for 5 min showed a marked collapse response [62.2±1.9% versus 29.7±3.5% in DMSO (Bay-61 vehicle), $P<0.01$]. As a control for inhibitor specificity and potential toxicity, the same treatment was applied to cells lacking the kinases. In this case, Syk inhibitor did not induce any changes in the percentage of collapsed cells compared with DMSO (28.3±1.7% versus 28.0±0.3%, respectively, $P>0.05$). To confirm these results and address the question of whether the collapse response depends on the level of Syk kinase activity, a dose-response experiment was performed using two Syk inhibitors, namely Bay-61 and Piceatannol. Percentages of collapsed growth cones were dose dependent (Fig. 5B, middle and right). Therefore, it appears that in cultured commissural neurons Syk is constitutively activated and that directly decreasing Syk kinase activity to a given level is sufficient to rapidly induce growth cone collapse. These results also suggest that Syk inhibition is a general requirement for growth cone collapse.

In a last set of experiments, EphB2/Syk interaction as well as the phosphorylation state of Syk upon ephrin B3 binding was examined on freshly isolated tissue fragments enriched in commissural neurons. As reported previously (Charoy et al., 2012; Nawabi et al., 2010), this approach has the advantage of allowing neurons to be assessed in their physiological context. EphB2 was immunoprecipitated and associated proteins were blotted with anti-Syk antibody (Fig. 5C). A band corresponding to highly phosphorylated Syk kinase (see upper

Development (2016) 143, 2183-2193 doi:10.1242/dev.128629

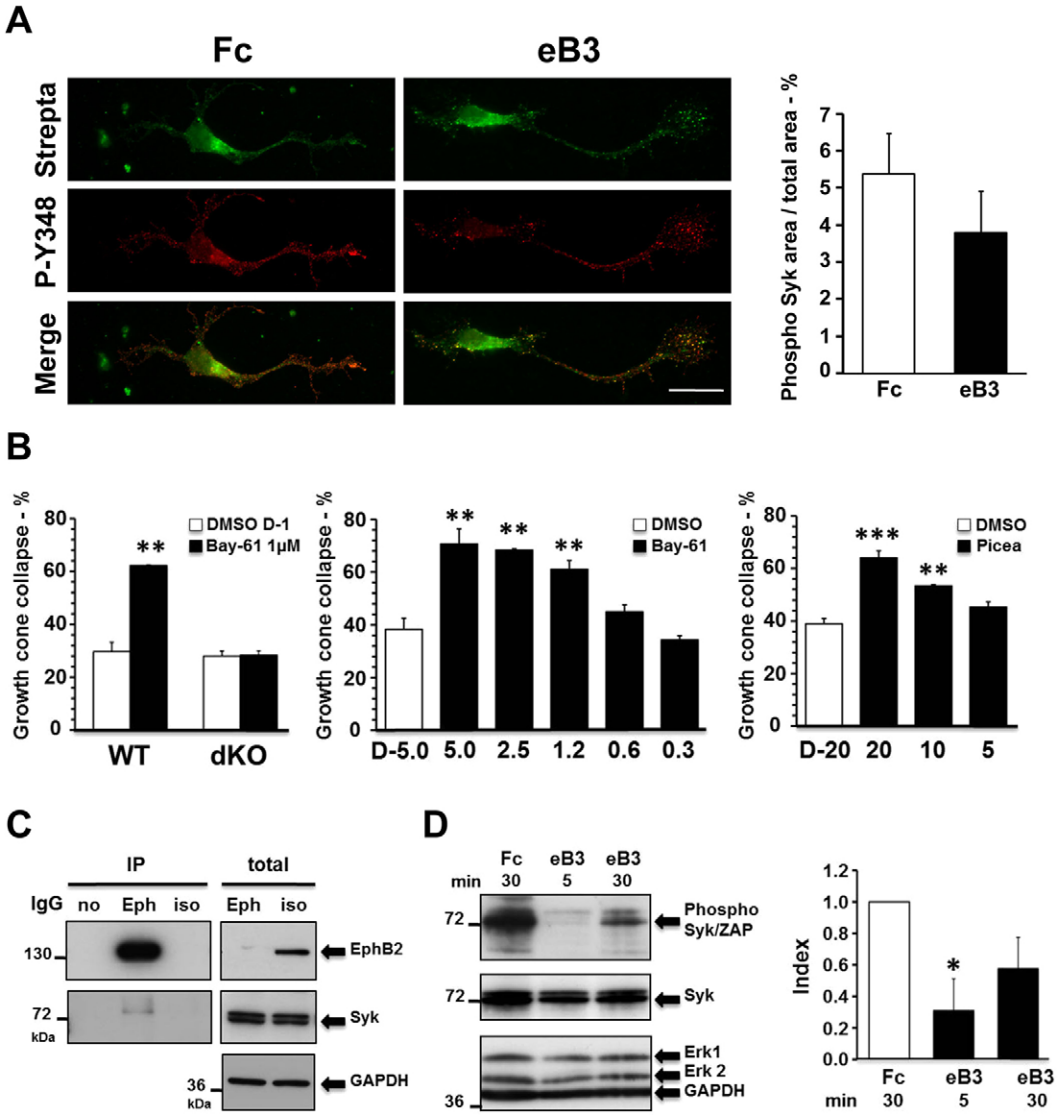

Fig. 5. Ephrin B3-induced collapse is associated with a decrease in Syk phosphorylation. (A) Commissural neurons cultured for 48 h were treated for 5 min with control Fc or eB3 at 2.5 µg/ml. Green labeling represents eB3 bound fraction (streptavidin, living cells) and red labeling represent phospho-Syk Y348 (permeabilized cells). Scale bars: 5 µm. Quantification of phospho-Syk signal intensities obtained from three independent experiments with more than 16 cells analyzed per condition are presented as mean percentage±s.e.m. (B) Cultures of commissural neurons derived from WT or dKO embryos were incubated for 5 min in the presence of Syk pharmacological inhibitors (Bay-61 and Piceatannol) at the indicated concentrations and the percentage of growth cone collapse was determined. As control for inhibitor vehicle, cells were treated with culture medium supplemented with DMSO (D-5.0 and D-20 correspond to control for Bay-61 5 µM and Piceatannol 20 µM, respectively). Experiments were performed in triplicate with at least 100 growth cones analyzed per coverslip and were repeated two or three times. Bar charts show the mean percentage±s.d. (C) EphB2 (Eph) was immunoprecipitated from tissue extracts and associated proteins were blotted with anti-EphB2, anti-Syk (clone 01) or anti-Gapdh antibodies. Omitted IgG (no) and isotype IgG (iso) conditions were used as controls. For total lysates, 30 µg protein, corresponding to 6% of IP extracts, was loaded on the gel. (D) Western blot analysis of phospho-Syk/Zap70 Y352/319 and Syk (clone 01) in tissue extracts treated with Fc or eB3. Erk1, Erk2 and Gapdh proteins were used as loading controls. Quantification of signal intensities obtained from three independent experiments is depicted as mean index±s.d. *P<0.05, **P<0.01, ***P<0.001. Two-tailed Student's t-test.

band in total lysates blotted with anti-Syk antibodies) was observed in EphB2 immunoprecipitate (IP, Eph) but not when IgG was omitted (no) or in isotype control IgG (iso) conditions, providing evidence of EphB2/Syk interaction. To examine the phosphorylation status of Syk upon ephrin B3 binding, fragments of commissural neuron-enriched tissues were incubated at 37°C with preclustered control Fc or eB3 and protein lysates were blotted with anti-phospho-Syk antibodies. eB3 treatment did not alter the level of Syk (Fig. 5D, middle). According to our previous observations on embryonic spinal cord sections (Fig. 1A,B) or freshly isolated tissues (Fig. 1D), Syk is present in phosphorylated forms in the control Fc condition. eB3 treatment decreased the Syk phosphorylation level, with a pronounced effect after 5 min incubation, whereas phospho-Syk was still diminished but to a lesser extent after 30 min (Fig. 5D). Thus, eB3 induced a rapid and probably reversible inhibition of Syk phosphorylation. Taken together, these results indicated that in commissural neurons Syk kinases are constitutively activated and that ephrin B3 induces growth cone collapse through Syk kinase inhibition.

Altogether, our results suggest a model whereby Syk kinases are activated in commissural axons at the precrossing stage but, upon floor plate crossing and exposure to midline cues, including ephrin B3, Syk kinases are dephosphorylated, allowing the repulsive

Development (2016) 143, 2183-2193 doi:10.1242/dev.128629

function of the floor plate to operate. Notably, because Syk dephosphorylation is likely to occur locally at the growth cone, it would not be detected on spinal cord sections by immunolabeling.

DISCUSSION

Syk activity and growth cone responsiveness to guidance cues

We have shown in this study that Syk kinases are required for ephrin B3-mediated commissural neuron growth cone collapse, and we collected data implicating EphB2 in this process. These findings extend our previous work performed on hippocampal neurons reporting that the ITAM-bearing CD3zeta molecule and associated Syk kinases are required for ephrin A1/EphA4-induced collapse (Angibaud et al., 2011). Although the use of two couples of ephrin/Eph lead to a similar outcome, major differences were observed between the two populations of neurons regarding the level of Syk phosphorylation and the kinetics of collapse. In hippocampal neurons, Syk phosphorylation was low at basal level and increased upon ephrin ligand binding; collapse was slow (45 min; Fig. S1) (Angibaud et al., 2011; Hatterer et al., 2011). By contrast, in commissural neurons, Syk phosphorylation was constitutively elevated and decreased upon ephrin binding, although the difference did not reach statistical significance; collapse was rapid (5 min). Furthermore, unlike hippocampal neurons, Eph clusters were preformed at basal level in commissural neurons. Altogether, these observations suggest that the Syk level of activation relies on Eph receptor clustering, which does not necessarily depend on ephrin ligand binding, and that collapse requires Syk to reach a threshold of activation. Such requirements could account for the slow and rapid collapse kinetics observed in these two populations. In support of this idea of an activation threshold, impacting Syk kinase activity through application of Syk pharmacological inhibitors resulted in distinct outcomes. Applied to hippocampal neurons in which, at basal level, Syk activation is under the threshold, Syk inhibitor had no collapsing effect per se. Moreover, by preventing the ephrin-induced increase of Syk activation, Syk inhibitor antagonized growth cone collapse. By contrast, applied on commissural neurons in which, at basal level, the activation threshold is essentially reached, Syk inhibitor readily induced collapse and the collapsing response relied on the relative level of Syk kinase activity. It is therefore tempting to speculate that Syk acts as a molecular switch of growth cone attractive and repulsive responses. Interestingly, in T cells, a graded and switchable Syk-dependent response to ephrins has been reported (Kawano et al., 2012). The authors described an ephrin concentration-dependent switch from promotion to inhibition of TCR-induced proliferation, with high concentrations of ephrin negatively impacting T cell proliferation. Notably, the switch was associated with strong Eph receptor activation and inhibition of the Src (Lck) and Syk (Zap70) kinase activities through the recruitment of the phosphatase Shp1 (Ptpn6) (Kawano et al., 2012).

Consistent with Syk kinases being downstream of Src kinases in ITAM-based signaling, simply decreasing Src activity using a pharmacological inhibitor is equally sufficient to induce growth cone collapse in commissural neurons (N.N., unpublished). Actually, whereas there is little evidence in the literature of Syk kinases determining growth cone behavior, a causal link between the Src state of activation and growth cone behavior has been elegantly demonstrated (Yam et al., 2009; Robles et al., 2005). These findings illustrate the graded and switchable nature of Src/Syk-dependent growth cone responses and fit well with the idea that coupling Syk kinase activation with inhibition constitutes an integrated molecular readout utilized by guidance molecules to change growth cone behavior.

Proper floor plate navigation relies on Syk kinases

We showed in this study that in navigating commissural axons Syk is phosphorylated when precrossing axons are attracted to the floor plate. However, by analyzing commissural axon trajectory in spinal cord open-book preparations of dKO embryos, we found that Syk kinases are dispensable for axon attraction to the midline but are required for proper exit. Importantly, consistent with the coordinated activation of Src/Syk kinases in ITAM-based signaling, similar results have been reported for Src kinases. Phospho-Src staining of spinal cord sections of mouse embryos revealed a Syk-like pattern of activation (Yam et al., 2009), and recent studies performed in *Drosophila* showed that Src family kinases are dispensable for midline attraction of commissural axons but antagonize midline crossing (O'Donnell and Bashaw, 2013). Whether this also applies to rodents remains to be determined, but these findings are nonetheless in agreement with *in vitro* data showing that Src/Syk kinases confer growth cone responsiveness to repulsive signals. However, they conflict somewhat with prevailing models positioning Src kinases downstream of guidance cues known to mediate attraction to the midline (i.e. netrin, Shh and VEGF) (Meriane et al., 2004; Ruiz de Almodovar et al., 2011; Yam et al., 2009).

Growth cone advance depends on the repeated formation and dissociation of transient contacts between adhesion molecules and the ECM or adjacent cells. Referred to as adhesion turnover, this process depends on tension forces created by physical links between adhesion molecules and the internal dynamics of the cytoskeletal network (Thoumine, 2008). Adhesion turnover can be schematically deconstructed into sequential phases. (1) The assembly phase consists of initial ligand-receptor binding and physical attachment to the cytoskeletal network, thus putting it under tension, and is associated with weak adhesion (slip bond). (2) The stabilization phase allows reinforcement of cytoskeleton-adhesion molecule links and is associated with strong adhesion (catch bond). (3) The disassembly phase, in which linkages between adhesion receptors and the cytoskeleton are dismantled or broken (Choquet et al., 1997; Thoumine, 2008). Several lines of data have provided evidence that, although recruited to the adhesion point, Src and Syk kinases are not necessary for adhesion assembly but rather play a role in adhesion stabilization and/or disassembly (Felsenfeld et al., 1999; Fincham and Frame, 1998; Suter and Forscher, 2001; Webb et al., 2004; Abram and Lowell, 2009; de Virgilio et al., 2004; Miranti et al., 1998). Therefore, in order to discuss the role of Src/Syk kinases in growth cone guidance, their involvement in adhesion turnover needs to be considered.

On the basis of what we have learned from the extended ITAM-based paradigm (i.e. its interplay with adhesion molecules) one can speculate that guidance cues that mediate attraction towards the midline increase the binding capability of growth cones, which in turn leads to downstream Src/Syk activation. By impacting on adhesion stabilization/disassembly, Src/Syk kinases could positively regulate the direction and speed of growth cone progression towards the midline. However, upon crossing, inhibitory signals intersect with activating signals, leading to Src/Syk inhibition and growth cone repulsion. Src kinases phosphorylate both immunoreceptor activation (ITAM) and inhibition (ITIM) motifs. ITIMs allow the recruitment of phosphatases such as Shp1, Shp2 (Ptpn11) or Ship (Inpp5d) that decrease the phosphorylation of various substrates, including those crucial in adhesion/migration (Bryceson et al., 2009; Oh et al., 1999; Pereira and Lowell, 2003; Underhill and Goodridge, 2007; Wang et al., 2013). The coordinated induction of activating and inhibitory molecules could act in an integrated manner to regulate the strength of adhesion. That said, in $Syk^{-/-}$; $Zap70^{-/-}$ animals, simple adhesion might be sufficient to relay the attractive properties of guidance cues;

Development (2016) 143, 2183-2193 doi:10.1242/dev.128629

the growth cone would still progress towards the midline, although at low speed. However, the fact that Syk activation might be a prerequisite to gain sensitivity to repulsive signals could account for midline repulsive defects observed in dKO animals.

Integration of guidance signals by ITAM-based signaling

We showed in this study that ephrins are obvious candidates in driving Syk-dependent switching at the midline. However, comparing the collapse response to Slit2/3 and to semaphorin 3B (Sema3B) in WT and dKO commissural neurons in culture, we found that both require signaling via Syk kinases (N.N., unpublished). These observations support the idea that the interpretation of signals emanating from diverse guidance cues as being repulsive relies on Syk kinase activity. Although all present at the midline, ephrin B3 and Slit2/3 or Sema3B plausibly act in different spatial and temporal windows. Expressed at the floor plate by glial cells, ephrin B3 acts with short-range activity, whereas Slit2/3 and Sema3B are secreted factors with potentially longer range activity. Combinations and sequences of ligand accessibility and guidance receptor availability are likely to play crucial roles in providing spatial and temporal coordination of guidance signals at the floor plate (Dickson and Zou, 2010; Kaplan et al., 2014; Nawabi and Castellani, 2011). In addition, the common use of Syk signaling would provide an efficient way to ensure the integration of the various guidance forces.

In conclusion, ITAM-based signaling might constitute an integrated molecular readout of environmental information allowing the proper coordination between attraction and repulsion in the context of a complex array of guidance cues.

MATERIALS AND METHODS

Animals

The generation and genotyping of mutant mice and animal procedures are described in supplementary Materials and Methods. Animal care and procedures were conducted according to European Community Council Directive 2010/63/UE and the French Ethical Committee.

Antibodies

Antibodies and reagents are described in Table S1.

DiI staining on spinal cord open-book preparations

Wild-type and mutant mouse embryos (E13.5) were collected in cold PBS and dissected in cold Hank's Balanced Salt Solution (HBSS), 6.5% glucose (Gibco). Neural tubes were isolated and prepared in an open-book preparation and then fixed in 4% paraformaldehyde (PFA) for 2 h and kept in PBS at 4°C. Four to eight small DiI crystals (Molecular Probes) were inserted in the most dorsal part of one hemicord to achieve anterograde labeling of commissural axons. The different trajectories summarized in Fig. 2A were observed after 48 h by conventional fluorescence microscopy and were categorized as 'normal', 'stalling', 'defective turning' and 'back crossing' phenotypes. DiI crystals label fiber tracts and, rarely, isolated fibers, and several fiber tracts with different trajectories can be labeled from one crystal. Since it was not possible to accurately count the number of fibers, we counted one for the ensemble of fiber tracts with a particular phenotype. For each open-book, the percentage of the different phenotypes was determined. For example, for dKO embryo number 7, seven crystals were placed and a total of 25 phenotypes were counted comprising seven normal (28%), ten stalling (40%), eight defective turning (32%) and zero back crossing (0%). Results are represented as the mean percentage±s.e.m. of the different phenotypes (n, the number of embryos analyzed) and for each phenotype the WT group was compared with the dKO group.

Primary culture of spinal cord commissural neurons

Commissural neurons were obtained from E12.5 spinal cord open-book preparations by dissecting the most dorsal part containing commissural neuron cell bodies in Neurobasal medium (Gibco). Tissues were then incubated in a mixture of trypsin (5 mg/ml) and DNase (0.1 mg/ml) at 37°C for 30 min and washed in Dulbecco's Modified Eagle Medium (DMEM) (Gibco) containing 10% fetal calf serum (FCS) (First Link). Cells were dissociated by trituration through Pasteur pipettes. The dissociated cells were plated onto coated glass coverslips (25 µg/ml poly-L-lysine and 20 µg/ml laminin; Sigma) at 26,000 cells/well in a 24-well plate. Commissural neurons were cultured in Neurobasal medium (Gibco) supplemented with 1% B27 (Gibco), 0.1 µg/ml netrin 1 (R&D Systems), 0.5 mM L-glutamine (Gibco), 50 U/ml penicillin (Gibco) and 50 µg/ml streptomycin (Gibco).

In vitro collapse assay

After 2 days in culture, commissural neurons were treated with control Fc or ephrin B3-Fc recombinant proteins (R&D Systems, Q15768, P01857) that had been previously preclustered with an anti-human Fc biotinylated antibody (Jackson ImmunoResearch) at a 1:2 ratio in plain Neurobasal medium for 2 h at room temperature (RT). Preclustered ephrin B3-Fc and control Fc or monomeric ephrin B3 (0.5 µg/ml) were bath applied and incubated at 37°C for the indicated period of time. In some experiments, commissural neurons were treated with the Syk inhibitors Bay-61 {2-[7-(3,4-dimethoxyphenyl) imidazo[1,2-c]pyrimidin-5-ylamino]pyridine-3-carboxamide hydrochloride} and Piceatannol {4-[(*E*)-2-(3,5-dihydroxyphenyl)ethenyl]benzene-1,2-diol} (Sigma-Aldrich) at the indicated concentrations for 5 min. As control for inhibitor, cells were treated with culture medium supplemented with vehicle DMSO. Neurons were then washed in PBS and fixed in 4% PFA, 2% sucrose for 10 min. Growth cones were visualized by polymerized actin staining using Alexa Fluor 488-phalloidin (Molecular Probes). Growth cones with two or fewer filopodia were considered as collapsed. The state of growth cones was scored under blinded condition.

Immunofluorescent labeling

On tissue sections

Tissue sections were obtained from E11-13 embryos as previously described (Hatterer et al., 2011). For immunostaining, sections were first incubated in blocking buffer PBS-T (0.3% Triton X-100) containing 3% BSA for 1 h at RT and then with primary antibodies overnight at 4°C. After three washes in PBS-T, sections were incubated with appropriate Alexa Fluor-conjugated antibodies diluted in blocking buffer for 1 h at RT. After three washes in PBS-T, sections were treated with 0.1 µg/ml DAPI (4′,6-diamidino-2-phenylindole dihydrochloride) for 5 min to label the nuclei and then mounted in Fluor Preserve reagent (Calbiochem). For control experiments, samples were treated following the same procedure but primary antibodies were omitted.

On cultured cells

Co-immunostaining of EphB2 receptor and ephrin B3 cell-bound fraction was performed on live cells. Commissural neurons were treated as described for the collapse assay with preclustered ephrin B3-Fc and control Fc (2.5 µg/ml) for 5 min at 37°C, washed in cold PBS and kept on ice. Cells were labeled for 15 min using goat anti-EphB2 antibody, washed and further incubated for 30 min with Alexa Fluor 488-conjugated anti-goat secondary antibody and Alexa Fluor 546-conjugated streptavidin to visualize the ephrin B3 cell-bound fraction. After washing, cells were fixed in 4% PFA for 10 min. Coverslips were mounted in Fluor Preserve reagent (Calbiochem).

To quantify the number of ephrin B3 clusters at the surface of growth cones, cells were treated in the same manner (5 min at 37°C), washed in cold PBS, fixed in 4% PFA, 2% sucrose for 10 min and incubated with Alexa Fluor 488-conjugated streptavidin for 30 min at RT. A region of interest (ROI) corresponding to the growth cone area was defined based on differential interference contrast (DIC) images, and the number of ephrin B3 clusters was quantified using ImageJ software (NIH). For individual growth cones, a threshold corresponding to three times the background value was chosen manually and the cluster number was determined using the 'analyze particles' function.

Co-immunostaining of ephrin B3 clusters present at the cell surface and phospho-Syk was performed sequentially. Cells treated as previously described (5 min at 37°C) were washed in cold PBS and fixed in 4% PFA, 2% sucrose. They were then permeabilized in blocking buffer for 1 h and exposed to rabbit anti-phospho-Syk Y348 antibodies overnight at 4°C. After washing in PSB-T,

Development (2016) 143, 2183-2193 doi:10.1242/dev.128629

cells were incubated with Alexa Fluor 488-conjugated streptavidin and Alexa Fluor 555-conjugated anti-mouse antibodies in blocking solution for 1 h at RT. To quantify phospho-Syk signal intensities, an ROI delimiting the cell surface was defined based on DIC images. Using ImageJ, a threshold corresponding to three times the average signal intensity of cells treated with control Fc was applied on each cell and the resulting values, corresponding to the total phospho-Syk-labeled area, were divided by the cell area.

To determine the percentage of Dcc^{+} cells and cell viability, commissural neurons cultured for 48 h were fixed in 4% PFA, 2% sucrose and labeled with anti-Dcc antibodies and DAPI (0.1 µg/ml). Cell viability was quantified based on DAPI nuclear staining. Cells with small, bright and pyknotic nuclei were counted as dead, whereas those with large and dim nuclei presenting visible nucleoli were counted as alive.

Images were acquired with a Zeiss Axio Imager.Z1 fluorescence microscope and analyzed using Axiovision software 4.7. Digitized images were processed for adjustment of brightness and contrast with ImageJ and Adobe Photoshop CS image editing software.

Western blots

Spinal cords from E12.5 embryos were prepared in an open-book configuration and the dorsal part was further dissected to isolate commissural neurons. Tissue fragments were lysed in buffer comprising 20 mM Tris-HCl pH 7.5, 150 mM NaCl, 1% NP-40, 60 mM octyl glucoside, protease and phosphatase inhibitors. For immunoprecipitations, precleared lysates containing 500 µg protein were incubated overnight with 2 µg anti-EphB2 or control IgG followed by 2 h with protein G-Sepharose beads (Millipore). After five washes in lysis buffer, pellets were resuspended in Laemmli buffer. In some experiments, tissue fragments were incubated with preclustered ephrin B3-Fc or control Fc at 2.5 µg/ml for 5 or 30 min at 37°C. After one wash in PBS, pellets were resuspended in Laemmli buffer. Proteins were resolved on 9% SDS-PAGE and transferred to nitrocellulose membranes (PerkinElmer Life Sciences). Membranes were blocked for 30 min in TBS-T (150 mM NaCl, 20 mM Tris, 0.1% Tween 20, pH 7.5) containing 5% milk and blotted overnight at 4°C with primary antibodies. After three washes in TBS-T, membranes were incubated for 1 h at RT with horseradish peroxidase-conjugated secondary antibodies (Amersham). Immunoreactive proteins were visualized using an enhanced chemiluminescence detection system (ThermoFisher Scientific). Phospho-Syk or phospho-EphB2 signal intensities were quantified using ImageJ and corrected for protein loading using Gapdh. Results are presented as index values relative to control conditions.

Statistical analyses

A Student's *t*-test (Microsoft Excel) was performed, except for results presented in Fig. 2C for the back crossing phenotype and Fig. 4C for which a Mann–Whitney test (AnaStats, www.anastats.fr) was applied.

Acknowledgements

We thank E. Schweighoffer and V. L. Tybulewicz (Division of Immune Cell Biology, MRC National Institute for Medical Research, London) for providing the $Syk^{+/-}$; $Zap70^{-/-}$ knockout mice; J. Falk (Inserm U1217 CNRS U5310, INMG, Lyon) for critically reading the manuscript; J. M. Vicat, J. Condoluci, A. Chamousset and M. Lavigne (Alecs, Faculté Rockfeller, Lyon) for animal care; and C. Bardel Danjean (CNRS UMR5588, Laboratoire de Biométrie et Biologie Evolutive, Villeurbanne) for statistical analyses.

Competing interests

The authors declare no competing or financial interests.

Author contributions

V.C. brought expertise on the model of axon guidance during spinal cord midline crossing. H.B., V.C., N.N. and V.P.-M. contributed to the formulation and design of the experiments. A.B., C.C., N.C., I.J., N.N., C.M., V.P.-M. and C.W. performed experiments or data analysis. N.N. and V.P.-M. wrote the manuscript with contributions from H.B., J.H. and mainly V.C.

Funding

This work was supported by Institut National de la Santé et de la Recherche Médicale (Inserm), Centre National de la Recherche Scientifique (CNRS), Université Claude Bernard Lyon 1 and Université de Nantes. The work of the team of V.C. was conducted within the framework of the Labex CORTEX and Labex DevWeCAN of Université de Lyon, within the program 'Investissements d'Avenir' [ANR-11-IDEX-0007] operated by the French National Research Agency [Agence Nationale de la Recherche (ANR)] and Fondation pour la Recherche Médicale (FRM).

Supplementary information

Supplementary information available online at
http://dev.biologists.org/lookup/suppl/doi:10.1242/dev.128629/-/DC1

References

Abram, C. L. and Lowell, C. A. (2007). The expanding role for ITAM-based signaling pathways in immune cells. *Sci. STKE* **2007**, re2.

Abram, C. L. and Lowell, C. A. (2009). The ins and outs of leukocyte integrin signaling. *Annu. Rev. Immunol.* **27**, 339-362.

Angibaud, J., Louveau, A., Baudouin, S. J., Nerrière-Daguin, V., Evain, S., Bonnamain, V., Hulin, P., Csaba, Z., Dournaud, P., Thinard, R. et al. (2011). The immune molecule CD3zeta and its downstream effectors ZAP-70/Syk mediate ephrin signaling in neurons to regulate early neuritogenesis. *J. Neurochem.* **119**, 708-722.

Angibaud, J., Baudouin, S. J., Louveau, A., Nerrière-Daguin, V., Bonnamain, V., Csaba, Z., Dournaud, P., Naveilhan, P., Noraz, N., Pellier-Monnin, V. et al. (2012). Ectopic expression of the immune adaptor protein CD3zeta in neural stem/progenitor cells disrupts cell-fate specification. *J. Mol. Neurosci.* **46**, 431-441.

Arvanitis, D. and Davy, A. (2008). Eph/ephrin signaling: networks. *Genes Dev.* **22**, 416-429.

Baudouin, S. J., Angibaud, J., Loussouarn, G., Bonnamain, V., Matsuura, A., Kinebuchi, M., Naveilhan, P. and Boudin, H. (2008). The signaling adaptor protein CD3{zeta} is a negative regulator of dendrite development in young neurons. *Mol. Biol. Cell* **19**, 2444-2456.

Boulanger, L. M. (2009). Immune proteins in brain development and synaptic plasticity. *Neuron* **64**, 93-109.

Brdicka, T., Kadlecek, T. A., Roose, J. P., Pastuszak, A. W. and Weiss, A. (2005). Intramolecular regulatory switch in ZAP-70: analogy with receptor tyrosine kinases. *Mol. Cell. Biol.* **25**, 4924-4933.

Bryceson, Y. T., Ljunggren, H. G. and Long, E. O. (2009). Minimal requirement for induction of natural cytotoxicity and intersection of activation signals by inhibitory receptors. *Blood* **114**, 2657-2666.

Charoy, C., Nawabi, H., Reynaud, F., Derrington, E., Bozon, M., Wright, K., Falk, J., Helmbacher, F., Kindbeiter, K. and Castellani, V. (2012). gdnf activates midline repulsion by Semaphorin3B via NCAM during commissural axon guidance. *Neuron* **75**, 1051-1066.

Choquet, D., Felsenfeld, D. P. and Sheetz, M. P. (1997). Extracellular matrix rigidity causes strengthening of integrin–cytoskeleton linkages. *Cell* **88**, 39-48.

Chuang, W. and Lagenaur, C. F. (1990). Central nervous system antigen P84 can serve as a substrate for neurite outgrowth. *Dev. Biol.* **137**, 219-232.

Davis, S., Gale, N. W., Aldrich, T. H., Maisonpierre, P. C., Lhotak, V., Pawson, T., Goldfarb, M. and Yancopoulos, G. D. (1994). Ligands for EPH-related receptor tyrosine kinases that require membrane attachment or clustering for activity. *Science* **266**, 816-819.

de Virgilio, M., Kiosses, W. B. and Shattil, S. J. (2004). Proximal, selective, and dynamic interactions between integrin alphaIIbbeta3 and protein tyrosine kinases in living cells. *J. Cell Biol.* **165**, 305-311.

Dickson, B. J. and Zou, Y. (2010). Navigating intermediate targets: the nervous system midline. *Cold Spring Harb. Perspect. Biol.* **2**, a002055.

Egea, J. and Klein, R. (2007). Bidirectional Eph–ephrin signaling during axon guidance. *Trends Cell Biol.* **17**, 230-238.

Felsenfeld, D. P., Schwartzberg, P. L., Venegas, A., Tse, R. and Sheetz, M. P. (1999). Selective regulation of integrin-cytoskeleton interactions by the tyrosine kinase *Src*. *Nat. Cell Biol.* **1**, 200-206.

Fincham, V. J. and Frame, M. C. (1998). The catalytic activity of Src is dispensable for translocation to focal adhesions but controls the turnover of these structures during cell motility. *EMBO J.* **17**, 81-92.

Funk, S. D. and Orr, A. W. (2013). Ephs and ephrins resurface in inflammation, immunity, and atherosclerosis. *Pharmacol. Res.* **67**, 42-52.

Hamada, J., Okumura, N., Inagaki, M., Taniguchi, H., Nakahata, Y., Sano, S.-i. and Nagai, K. (2004). Tyrosine phosphorylation of BIT on photic stimulation in the rat retina. *FEBS Lett.* **557**, 204-208.

Hatterer, E., Benon, A., Chounlamountri, N., Watrin, C., Angibaud, J., Jouanneau, E., Boudin, H., Honnorat, J., Pellier-Monnin, V. and Noraz, N. (2011). Syk kinase is phosphorylated in specific areas of the developing nervous system. *Neurosci. Res.* **70**, 172-182.

Imondi, R., Wideman, C. and Kaprielian, Z. (2000). Complementary expression of transmembrane ephrins and their receptors in the mouse spinal cord: a possible role in constraining the orientation of longitudinally projecting axons. *Development* **127**, 1397-1410.

Ivashkiv, L. B. (2009). Cross-regulation of signaling by ITAM-associated receptors. *Nat. Immunol.* **10**, 340-347.

Jakus, Z., Fodor, S., Abram, C. L., Lowell, C. A. and Mócsai, A. (2007). Immunoreceptor-like signaling by beta 2 and beta 3 integrins. *Trends Cell Biol.* **17**, 493-501.

Janes, P. W., Nievergall, E. and Lackmann, M. (2012). Concepts and consequences of Eph receptor clustering. *Semin. Cell Dev. Biol.* **23**, 43-50.
Jevince, A. R., Kadison, S. R., Pittman, A. J., Chien, C.-B. and Kaprielian, Z. (2006). Distribution of EphB receptors and ephrin-B1 in the developing vertebrate spinal cord. *J. Comp. Neurol.* **497**, 734-750.
Kadison, S. R., Mäkinen, T., Klein, R., Henkemeyer, M. and Kaprielian, Z. (2006). EphB receptors and ephrin-B3 regulate axon guidance at the ventral midline of the embryonic mouse spinal cord. *J. Neurosci.* **26**, 8909-8914.
Kadlecek, T. A., van Oers, N. S., Lefrancois, L., Olson, S., Finlay, D., Chu, D. H., Connolly, K., Killeen, N. and Weiss, A. (1998). Differential requirements for ZAP-70 in TCR signaling and T cell development. *J. Immunol.* **161**, 4688-4694.
Kaifu, T., Nakahara, J., Inui, M., Mishima, K., Momiyama, T., Kaji, M., Sugahara, A., Koito, H., Ujike-Asai, A., Nakamura, A. et al. (2003). Osteopetrosis and thalamic hypomyelinosis with synaptic degeneration in DAP12-deficient mice. *J. Clin. Invest.* **111**, 323-332.
Kaplan, A., Kent, C. B., Charron, F. and Fournier, A. E. (2014). Switching responses: spatial and temporal regulators of axon guidance. *Mol. Neurobiol.* **49**, 1077-1086.
Kawano, H., Katayama, Y., Minagawa, K., Shimoyama, M., Henkemeyer, M. and Matsui, T. (2012). A novel feedback mechanism by Ephrin-B1/B2 in T-cell activation involves a concentration-dependent switch from costimulation to inhibition. *Eur. J. Immunol.* **42**, 1562-1572.
Kazerounian, S., Duquette, M., Reyes, M. A., Lawler, J. T., Song, K., Perruzzi, C., Primo, L., Khosravi-Far, R., Bussolino, F., Rabinovitz, I. et al. (2011). Priming of the vascular endothelial growth factor signaling pathway by thrombospondin-1, CD36, and spleen tyrosine kinase. *Blood* **117**, 4658-4666.
Kitano, J., Kimura, K., Yamazaki, Y., Soda, T., Shigemoto, R., Nakajima, Y. and Nakanishi, S. (2002). Tamalin, a PDZ domain-containing protein, links a protein complex formation of group 1 metabotropic glutamate receptors and the guanine nucleotide exchange factor cytohesins. *J. Neurosci.* **22**, 1280-1289.
Letellier, E., Kumar, S., Sancho-Martinez, I., Krauth, S., Funke-Kaiser, A., Laudenklos, S., Konecki, K., Klussmann, S., Corsini, N. S., Kleber, S. et al. (2010). CD95-ligand on peripheral myeloid cells activates Syk kinase to trigger their recruitment to the inflammatory site. *Immunity* **32**, 240-252.
Long, H., Sabatier, C., Le Ma, C., Plump, A., Yuan, W., Ornitz, D. M., Tamada, A., Murakami, F., Goodman, C. S. and Tessier-Lavigne, M. (2004). Conserved roles for Slit and Robo proteins in midline commissural axon guidance. *Neuron* **42**, 213-223.
Luckashenak, N. and Clements, J. L. (2007). Signaling mechanisms utilized by antigen receptors and integrins: common intermediates, different outcomes? *Front. Biosci.* **12**, 419-436.
Mendes-da-Cruz, D. A., Stimamiglio, M. A., Munoz, J. J., Alfaro, D., Terra-Granado, E., Garcia-Ceca, J., Alonso-Colmenar, L. M., Savino, W. and Zapata, A. G. (2012). Developing T-cell migration: role of semaphorins and ephrins. *FASEB J.* **26**, 4390-4399.
Meriane, M., Tcherkezian, J., Webber, C. A., Danek, E. I., Triki, I., McFarlane, S., Bloch-Gallego, E. and Lamarche-Vane, N. (2004). Phosphorylation of DCC by Fyn mediates Netrin-1 signaling in growth cone guidance. *J. Cell Biol.* **167**, 687-698.
Miranti, C. K., Leng, L., Maschberger, P., Brugge, J. S. and Shattil, S. J. (1998). Identification of a novel integrin signaling pathway involving the kinase Syk and the guanine nucleotide exchange factor Vav1. *Curr. Biol.* **8**, 1289-1299.
Nawabi, H. and Castellani, V. (2011). Axonal commissures in the central nervous system: how to cross the midline? *Cell. Mol. Life Sci.* **68**, 2539-2553.
Nawabi, H., Briancon-Marjollet, A., Clark, C., Sanyas, I., Takamatsu, H., Okuno, T., Kumanogoh, A., Bozon, M., Takeshima, K., Yoshida, Y. et al. (2010). A midline switch of receptor processing regulates commissural axon guidance in vertebrates. *Genes Dev.* **24**, 396-410.
O'Donnell, M. P. and Bashaw, G. J. (2013). Src inhibits midline axon crossing independent of Frazzled/Deleted in Colorectal Carcinoma (DCC) receptor tyrosine phosphorylation. *J. Neurosci.* **33**, 305-314.
Ogawa, M., Miyakawa, T., Nakamura, K., Kitano, J., Furushima, K., Kiyonari, H., Nakayama, R., Nakao, K., Moriyoshi, K. and Nakanishi, S. (2007). Altered sensitivities to morphine and cocaine in scaffold protein tamalin knockout mice. *Proc. Natl. Acad. Sci. USA* **104**, 14789-14794.
Oh, E.-S., Gu, H., Saxton, T. M., Timms, J. F., Hausdorff, S., Frevert, E. U., Kahn, B. B., Pawson, T., Neel, B. G. and Thomas, S. M. (1999). Regulation of early events in integrin signaling by protein tyrosine phosphatase SHP-2. *Mol. Cell. Biol.* **19**, 3205-3215.
Pasquale, E. B. (2005). Eph receptor signalling casts a wide net on cell behaviour. *Nat. Rev. Mol. Cell Biol.* **6**, 462-475.
Pasquale, E. B. (2008). Eph-ephrin bidirectional signaling in physiology and disease. *Cell* **133**, 38-52.
Pereira, S. and Lowell, C. (2003). The Lyn tyrosine kinase negatively regulates neutrophil integrin signaling. *J. Immunol.* **171**, 1319-1327.
Pitulescu, M. E., Schmidt, I., Benedito, R. and Adams, R. H. (2010). Inducible gene targeting in the neonatal vasculature and analysis of retinal angiogenesis in mice. *Nat. Protoc.* **5**, 1518-1534.
Robles, E., Woo, S. and Gomez, T. M. (2005). Src-dependent tyrosine phosphorylation at the tips of growth cone filopodia promotes extension. *J. Neurosci.* **25**, 7669-7681.
Ruiz de Almodovar, C., Fabre, P. J., Knevels, E., Coulon, C., Segura, I., Haddick, P. C. G., Aerts, L., Delattin, N., Strasser, G., Oh, W.-J. et al. (2011). VEGF mediates commissural axon chemoattraction through its receptor Flk1. *Neuron* **70**, 966-978.
Sharfe, N., Nikolic, M., Cimpeon, L., Van De Kratts, A., Freywald, A. and Roifman, C. M. (2008). EphA and ephrin-A proteins regulate integrin-mediated T lymphocyte interactions. *Mol. Immunol.* **45**, 1208-1220.
Smith-Garvin, J. E., Koretzky, G. A. and Jordan, M. S. (2009). T cell activation. *Annu. Rev. Immunol.* **27**, 591-619.
Suter, D. M. and Forscher, P. (2001). Transmission of growth cone traction force through apCAM-cytoskeletal linkages is regulated by Src family tyrosine kinase activity. *J. Cell Biol.* **155**, 427-438.
Thoumine, O. (2008). Interplay between adhesion turnover and cytoskeleton dynamics in the control of growth cone migration. *Cell. Adh. Migr.* **2**, 263-267.
Turner, M., Mee, P. J., Costello, P. S., Williams, O., Price, A. A., Duddy, L. P., Furlong, M. T., Geahlen, R. L. and Tybulewicz, V. L. J. (1995). Perinatal lethality and blocked B-cell development in mice lacking the tyrosine kinase Syk. *Nature* **378**, 298-302.
Underhill, D. M. and Goodridge, H. S. (2007). The many faces of ITAMs. *Trends Immunol.* **28**, 66-73.
Wang, J., Shiratori, I., Uehori, J., Ikawa, M. and Arase, H. (2013). Neutrophil infiltration during inflammation is regulated by PILRalpha via modulation of integrin activation. *Nat. Immunol.* **14**, 34-40.
Webb, D. J., Donais, K., Whitmore, L. A., Thomas, S. M., Turner, C. E., Parsons, J. T. and Horwitz, A. F. (2004). FAK-Src signalling through paxillin, ERK and MLCK regulates adhesion disassembly. *Nat. Cell Biol.* **6**, 154-161.
Xu, H.-p., Chen, H., Ding, Q., Xie, Z.-H., Chen, L., Diao, L., Wang, P., Gan, L., Crair, M. C. and Tian, N. (2010). The immune protein CD3zeta is required for normal development of neural circuits in the retina. *Neuron* **65**, 503-515.
Yam, P. T., Langlois, S. D., Morin, S. and Charron, F. (2009). Sonic hedgehog guides axons through a noncanonical, Src-family-kinase-dependent signaling pathway. *Neuron* **62**, 349-362.
Yamada, M., Takeshita, T., Miura, S., Murata, K., Kimura, Y., Ishii, N., Nose, M., Sakagami, H., Kondo, H., Tashiro, F. et al. (2001). Loss of hippocampal CA3 pyramidal neurons in mice lacking STAM1. *Mol. Cell. Biol.* **21**, 3807-3819.
Zhang, J., Billingsley, M. L., Kincaid, R. L. and Siraganian, R. P. (2000). Phosphorylation of Syk activation loop tyrosines is essential for Syk function: an in vivo study using a specific anti-Syk activation loop phosphotyrosine antibody. *J. Biol. Chem.* **275**, 35442-35447.
Zou, Y., Stoeckli, E., Chen, H. and Tessier-Lavigne, M. (2000). Squeezing axons out of the gray matter: a role for slit and semaphorin proteins from midline and ventral spinal cord. *Cell* **102**, 363-375.

Supplementary Materials and Methods

Mice and genotyping

Wild-type C57BL/6 mice (Janvier Montpellier, France) were used in this study. *Syk* heterozygous and *Zap70* homozygous mutant mice (*Syk*$^{+/-}$; *Zap70*$^{-/-}$), on a C57BL/6 background (at least 10 backcrossing), were a kind gift from V. L. Tybulewicz (Division of Immune Cell Biology, MRC National Institute for Medical Research, London). Homozygous double-mutant embryos lacking both Syk and Zap70 (*Syk*$^{-/-}$; *Zap70*$^{-/-}$) were generated by crossing *Syk*$^{+/-}$; *Zap70*$^{-/-}$ mice. Embryos were genotyped by PCR. For the wild-type *Syk* allele we used primers a (5′-AGAGAAGCCCTGCCCATGGAC-3′) and b (5′-GTCCAGGTAGACCTCTTTGGGC-3′) and for the mutant *Syk* allele we used primers b and c (5′-GAGACTAGTGAGACGTGCT-3′). For *Zap70*, primers a (5′-GCACATATGCACTGTCCCTGGTCTA-3′) and c (5′-GGGTCGCTGTAGGGACTCTCGTACA-3′) were used for the wild-type allele and primers a and b (5′-TGGCTACCCGTGATATTGCTGAAGA-3′) were used for the mutated allele. Pregnant mice were sacrificed under deep anesthesia induced by halothane inhalation and the embryos were taken out by Caesarean section at the indicated day of gestation, the day of conception corresponding to E0.5. Mice were bred and maintained in Transgenic Animal Care Facility (ALECS) in Lyon, France. Animal care and procedures have been conducted according to the European Community Council Directive 2010/63/UE and the French Ethical Committee.

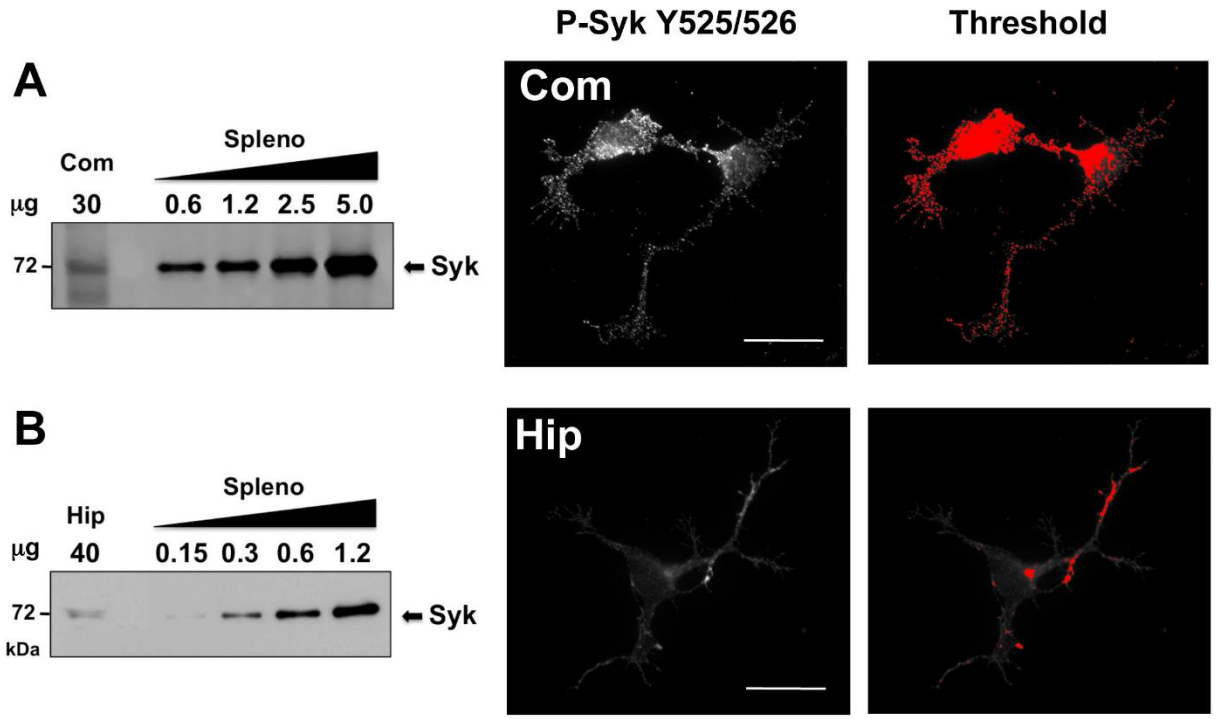

Fig. S1

Syk and phospho-Syk levels in commissural neurons (A) and hippocampal neurons (B). Syk level of expression was analyzed by Western-blots performed on freshly isolated cells obtained from the dorsal part of E12.5 open-book preparations (Com), from the hippocampus of E18 embryos (Hip) or from the spleen of adult mice (Spleno). Gels were loaded with the indicated quantities of proteins and membranes were blotted with anti-Syk Ab (N19). Syk levels of expression in commissural neurons and hippocampal neurons were estimated by semi quantitative immunoblot analysis at respectively 19.4±1.2 and 24.6±2.1 fold lower than that of splenocytes, which express a fair amount of the protein. Phospho-Syk level in those two populations of neuronal cells was assessed by immunolabeling on cultured cells, after 3 days for hippocampal neurons and 2 days for commissural neurons, using an anti-P-Syk Y5256/526 Ab. As illustrated, commissural neurons presented at basal level consistently higher phospho-Syk that hippocampal neurons. Scale bar: 20µm.

Table S1: Primary and secondary antibodies and reagents. IF: Immunofluorescence; WB: Western Blot; IP: Immunoprecipitation; C: used for Ctr-Fc and ephrinB3-Fc recombinant proteins preclusterization at a concentration ratio of 1 (recombinant proteins) for 2 (biotinylated anti-human).

Antibodies	**Species**	**Reference**	**Use**	**Dilution**
Syk (N-19)	Rabbit	Santa Cruz Biotechnology SC-1077	IF	1/100
Syk (clone 01)	Mouse	BioLegend #626201	WB	1/1000
Phospho-Syk Y525/526	Rabbit	Cell Signaling #2711	IF	1/300
Phospho-Syk Y348	Mouse	BD Biosciences #558167	IF	1/100
Phospho-ZAP Y319-Syk Y352	Rabbit	Cell Signaling #2701	IF	1/100
			WB	1/1000
EphB2	Goat	R&D Systems AF467	IF	1/100
			WB	1/1000
			IP	2µg
βIII tubulin	Mouse	Sigma Aldrich T8660	IF	1/3000
Phospho-EphB2 Y594	Rabbit	Abcam ab61791	WB	1/1000
Control IgG	Goat	Life Technologies #02-6202	IP	2µg
DCC	Mouse	BD Biosciences #554223	IF	1/500
Erk1/2	Rabbit	Cell Signaling #9102	WB	1/1000
GAPDH	Mouse	Millipore MAB374	WB	1/10000
Alexa Fluor 488/555 anti-mouse	Goat	Molecular Probes A10684/A21427	IF	1/2000
Alexa Fluor 488/555 anti-rabbit	Goat	Molecular Probes A11034/A21430	IF	1/2000
Alexa Fluor 488 anti-goat	Donkey	Molecular Probes A11055	IF	1/1000
HRP conjugated anti-mouse/rabbit	Goat	Jackson I. #115-036-003, # 111-036-003	WB	1/10000
Biotinylated anti-human	Donkey	Jackson I. #115-065-008	C	

Reagents			
Alexa Fluor 488-phalloïdin	Molecular Probes A12379	IF	1/40
Streptavidin Alexa Fluor 488	Molecular Probes S11223	IF	1/700
Streptavidin Alexa Fluor 546	Molecular Probes S11225	IF	1/700